

Relaxation of Hot Electrons in One-Dimensional Nanostructures Via LO-Phonon Emission

Vera Beatriz Campos

*Departamento de Física, Universidade Federal de São Carlos
Caixa Postal 676, 13565-905 São Carlos, S.P., Brasil*

and

Sankar Das Sarma

Department of Physics, University of Maryland, College Park, MD, USA

Received July 12, 1993

The presence of large electric fields can cause a substantial electron heating in small semiconductor devices. This effect can also occur with the application of a laser pulse, when the electrons become optically excited. In order to return to the equilibrium, these hot electrons must lose the excess energy to their surroundings (the cold lattice). In this work we have developed a theoretical study for the energy loss rate of one-dimensionally confined hot electrons to LO-phonons, in polar semiconductor quantum wires. Calculations are done for a model in which we assume the validity of the electron temperature model, describing the hot electron gas by a Fermi distribution function at a temperature $T > T_L$. We consider only the intrasubband relaxation within the lowest one dimensional subband, neglecting by now the effects of higher subbands. All the relevant physics is taken into account, including several mechanisms such as degeneracy, dynamic and static screening quantum confinement and hot phonon bottleneck effect. The effects of phonon confinement are also included, using two macroscopic models, the mechanical and the electrostatic models, which differ through the way boundary conditions are applied. The values for the energy loss calculated for the bulk phonon modes range between the results obtained for both confined models. We find that the guided (mechanical) modes produce more than an order magnitude slower energy relaxation than the slab (electrostatic) or the bulk modes. Our results show also that in the experimentally interesting electron temperature range of 50-200 K, the hot phonon effect is the single most important physical mechanism in our calculation.

I. Introduction

The investigation of the loss of the energy of the hot electrons in polar semiconductors has attracted a large amount of experimental and theoretical efforts, mainly in two and three dimensional systems^[1,2]. More recently, one dimensional hot electron relaxation has been studied theoretically^[3-7], stimulated by the fact that samples of one dimensional GaAs quantum-well-wires (QWW) with only the lowest subband occupied have been successfully grown^[8].

The actual situation for energy relaxation even for a single electron is somewhat complex. This is due to the fact that the longitudinal optical (LO) phonon, by itself, does not take energy out of the combined elec-

tron plus lattice system. The energy transfer from the source (electrical or optical field) to the surrounding environment occurs in four steps: (i) the electrons gain energy from the source, (ii) they lose energy by emitting acoustic and LO phonons, (iii) the LO-phonon decays into acoustic phonon via anharmonic processes, and finally, (iv) the lattice thermalizes with the surrounding heat bath, producing a net energy dissipation from the coupled electron-phonon system. The most efficient energy-relaxation process for the hot-electron gas, except at very low temperatures ($T < 30-40\text{K}$), is to emit LO phonons,

since the polar electron - LO-phonon Frohlich coupling is significantly stronger than the electron - acoustic-phonon deformation potential. At low electron tem-

peratures, very few hot electrons have enough energy to emit LO-phonons, which in bulk GaAs have an energy of 420K.

In the study of electron energy loss due to LO-phonon emission, there are two important time scales that should be considered: the electron equilibration time τ_e , and the electron-phonon scattering time τ_i . The first one corresponds to the scattering of the electrons with other electrons and with (immobile) impurities, which does not change the energy of the electron gas as a whole, although it may change the distribution of the energy and momentum of the electrons and take the electron gas towards an equilibrium spherical distribution. On the other hand, the inelastic electron-phonon scattering time, τ_i , represents the processes through which the electron gas actually loses energy to lattice excitations. When $\tau_e \ll \tau_i$ we can assume the electron gas to be in internal equilibrium during the entire energy-loss process. In the experiments we are interested in, the equilibrium of the electrons takes place on a 100-femtoseconds time scale while the typical values for energy loss to the lattice are of the order of picoseconds. This indicates that the adiabatic approximation of considering the electron gas to be in internal equilibrium during the entire energy-loss process at an electron temperature which is higher than the lattice temperature is adequate for our study. There is a third time scale relevant to this problem the so called hot-phonon lifetime τ_{ph} , which corresponds to the time scale in which the emitted LO-phonons decay into thermal acoustic phonons. τ_{ph} therefore controls the possibility of the emitted LO-phonons to be reabsorbed by the electrons before the LO-phonons can decay into acoustic phonons. The importance of the hot phonon effect depends on the relative magnitudes of τ_{ph} and the energy relaxation time τ for a single electron. When $\tau < \tau_{ph}$ the process of phonon reabsorption cannot be neglected and brings about a significant reduction in the power loss. For bulk GaAs, τ_{ph} is experimentally known^[9] to be several picoseconds, and τ is usually less than 1 ps, what indicates that this phonon bottleneck process must be included in any hot electron energy

relaxation calculation.

II. Theory

We calculate the energy loss per particle via intrasubband relaxation for a system of electrons confined by infinite square well potentials in a GaAs QWW of finite rectangular cross section of dimensions L_y and L_z . The electron-temperature model and the standard finite-temperature random phase approximation (RPA) were assumed to describe electronic response. The real lattice temperature is taken to be zero, but because the LO-phonons in GaAs correspond to a rather high temperature of 420K, our results should be valid for lattice temperatures up to 10-15K. We have taken into account in our work all the relevant physics, including several mechanisms such as degeneracy, dynamic and static screening, quantum confinement and hot phonon bottleneck effect. We have also included the effects of phonon confinement^[5,6], with the help of two prevailing macroscopic models: the electrostatic or slab model^[10] and the mechanical or guided model^[11]. We will restrict this study to n-doped QWW, with the electrons near the bottom of the conduction band, and with only the lowest electron subband occupied. This is justified for wire widths of less than 200Å, in the range of the electronic densities of $10^4 - 10^6 \text{ cm}^{-3}$. The electronic conduction band is assumed to be isotropic and parabolic, defined by a band effective mass m . This approximation is valid for most III-V semiconductor materials, provided that the electron energy is not too high ($< 200 \text{ meV}$ in the case of GaAs). Also, we will consider only the situation in which there are few holes in the valence band. This assumption is reasonable for experiments involving heating of doped semiconductors via electric field, but it is not necessarily valid when the electrons are excited in an undoped semiconductor by a laser pulse. The holes in the valence band could be treated in a way similar to that developed for electrons in this paper.

The electron gas is assumed to have attained quasi-equilibrium with itself at an electron temperature T which is higher than the surrounding lattice tempera-

ture T_L . We consider electron temperatures low enough as compared with the dispersionless LO-phonon energy ($k_B T < \hbar\omega_{LO}$) so that only the one-phonon emission process is significant. At equilibrium, the single electron will be at the bottom of the conduction band ($\mathbf{k} = \mathbf{0}$), where the energy is minimum. In an empty band of a polar material, for the temperature range $30K < T < 500K$, the only available mechanism by which the electron can lose energy is the LO-phonon emission. This emission continues until it is forbidden by energy conservation, i.e., until the electron has decayed to a level which is less than $\hbar\omega_{LO}$ from the bottom of the conduction band ($E < \hbar\omega_{LO}$). For even lower temperatures, acoustic phonons may play an important quantitative role, but the electronic coupling to acoustic phonons (via the deformation potential or the piezoelectric coupling) is substantially weaker than the polar Fröhlich coupling what makes the energy loss rates much lower^[9].

The energy relaxation rate is calculated using Fermi's "golden rule"^[12]. For the LO-phonon emission, the relevant interaction is the long-range Fröhlich interaction. The bulk LO-phonon emission relaxation times for a single electron have been calculated for 3D^[12] and 2D^[13] systems, and the results are of the order of one tenth of a picosecond. In a quasi 2D heterostructure or quantum well, the finite electronic wavefunction width in the third dimension reduces the scattering rate from the strictly 2D result, making the relaxation time for a real layer somewhat larger (10-40%).

II.1. Classical system

Let us first examine the simplest model, which consists of a system of non-interacting hot electrons at an electron temperature T , in contact with a lattice at temperature T_L and obeying a non-degenerate classical statistics (i.e., Maxwell-Boltzmann statistics). This model is appropriate for a low density electron gas at high temperatures ($k_B T \gg E$). We will consider here only the case where $T \gg T_L$, so that the MB factor at the lattice temperature can be neglected as compared with the electronic factor. This model will be referred

to as the classical model, although it uses the quantum interaction matrix element, as will be seen later.

For electrons obeying a classical MB distribution at a temperature $\mathcal{Z} = (k_B T)^{-1}$ the total power loss per electron due to LO phonon emission, ($E \geq \hbar\omega_{LO}$), can be written as

$$P_{mn} = \sqrt{\frac{\beta}{\pi}} \omega_{LO} \epsilon^{-\beta \hbar\omega_{LO}} \int_0^\infty dx e^{-\beta x} [x(x + \hbar\omega_{LO})]^{-1/2} [M^2(x_+) + M^2(x_-)] \quad (1)$$

where $M(x)$ is the Fröhlich matrix element for the specific one-dimensional electron-phonon-interaction, obtained from a quantum hamiltonian, the energies are given in units of Rydberg and we have defined $x \equiv (E - \hbar\omega_{LO})$ and $x_{\pm} \equiv (x \pm \hbar\omega_{LO})^{1/2} \pm x^{1/2}$. Since we are using classical statistics we are not considering the Pauli exclusion principle which requires that the transition is possible only when the final state is unoccupied. We are taking into account only single LO-phonon emission processes, which is justified because the adimensional Fröhlich coupling constant defined as $\alpha = e^2(2\hbar^3\omega_{LO}/m)^{-1/2}(\epsilon_\infty^{-1} - \epsilon_0^{-1})$ is much smaller than unity in the materials of our interest ($\alpha \simeq 0.07$ for GaAs)^[14].

For one-dimensional systems, the integral of Eq.(1) has to be performed numerically. However, for 2D and 3D systems the corresponding results can be obtained analytically and are of the general exponential form $P = (\hbar\omega_{LO}/\tau)e^{-\beta\hbar\omega_{LO}}$, where the relaxation time τ is $(\pi\alpha\omega_{LO})^{-1}$ in the 2D case and $(2\alpha\omega_{LO})^{-1}$ in 3D. For GaAs, one finds $\tau = 0.08ps$ (2D) and $0.13ps$ (3D).

Although this simple model for energy relaxation is strictly valid only for a low density electron gas at high temperatures, it provides a qualitatively correct description for hot electron energy relaxation in two and three dimensional systems^[2].

II.2. Quantum treatment

For the purpose of the energy relaxation problem, the total Hamiltonian for the system can be written as $H = H_0 + H_{e-ph}$, where the "unperturbed" part is $H_0 = H_e + H_{e-\epsilon} + H_{ph}$. The electron-phonon term,

which is responsible for the dissipation of energy from the electronic system, is considered to be a small perturbation to H_0 and can be expressed as

$$H_{e-ph} = \sum_{\mathbf{Q}} (M_{\mathbf{q}} \rho_{-\mathbf{q}} a_{\mathbf{Q}} + M_{\mathbf{q}}^* \rho_{\mathbf{q}} a_{\mathbf{Q}}^\dagger); \quad (2)$$

where $M_{\mathbf{q}}$ is the electron-phonon interaction matrix element, calculated for the one-dimensional system considered; $\mathbf{Q} = (q, q_{\perp})$ is the three-dimensional phonon wave-vector, with \mathbf{q} and \mathbf{q}_{\perp} respectively parallel and perpendicular to the QWW axis; $a_{\mathbf{Q}}$ and $a_{\mathbf{Q}}^\dagger$ are the creation and annihilation operators for an LO-phonon with wave-vector \mathbf{Q} and $\rho_{\mathbf{q}}$ is the Fourier transform of the electron density operator.

For an infinite well potential, the 1D electron wave function for the (r, s) state has the well known form

$$|k, r, s\rangle = 2V^{-1/2} \cos\left(\frac{r\pi y}{L_y}\right) \cos\left(\frac{s\pi z}{L_z}\right) \exp(ikx) \quad (3)$$

where V is the 3D volume of the system, and $-L_y \leq 2y \leq L_y$, and $-L_z \leq 2z \leq L_z$.

For the QWW system, the matrix element for the electron-phonon interaction can be written as

$$M_{\mathbf{q}}^2 = 2\alpha \left(\frac{\hbar^2}{2m}\right)^{1/2} (\hbar\omega_{LO})^{3/2} F(q, L_y, L_z) \quad (4)$$

where α is the Fröhlich coupling constant and $F(q, L_y, L_z)$ is the electronic form factor associated with the subband quantization in the x direction. This factor includes the specific geometry and boundary conditions of the system and will be discussed later.

The expression for the power loss per carrier for a system of hot electrons and bare phonons, for $T_L \ll T$, can be written as

$$P = -\frac{2}{N} \omega_{LO} [n_T(\omega_{LO}) - n_T(\omega_{LO})] \sum_{\mathbf{q}} R_{\mathbf{q}} \quad (5)$$

where n_T is the Bose factor and

$$R_{\mathbf{q}} = -\frac{2}{\hbar} M_{\mathbf{q}}^2 \text{Im} \chi(q, \omega_{LO}).$$

This equation for the total power loss contains the indirect effects of electron-electron interaction through the

retarded polarizability function, which, within the RPA is given by $\chi(q, \omega) = \chi(q, \omega)/\epsilon(q, \omega)$. The electronic dielectric function is $\epsilon(q, \omega) = 1 - \varphi(q)\chi^0(q, \omega)$, $\varphi(q)$ being the 1D Coulomb interaction in the lowest subband representation which includes the form factor for the system. The finite temperature bare polarizability $\chi^0(q, \omega; \mathbf{T}, \mu)$ can be obtained^[15] using the identity

$$\chi^0(q, \omega; T, \mu) = \int_0^\infty \frac{d\mu'}{4k_B T} \frac{\chi^0(q, \omega; T=0, \mu')}{\cosh^2[(\mu(T) - \mu')/2k_B T]}. \quad (6)$$

The chemical potential $\mu(T)$ is calculated numerically^[6] from the total electron density of the system and the free-electron polarizability at zero temperature is given by the bare bubble diagram^[16]. $\text{Im} \chi^0(q, \omega; \mathbf{T}=0)$ is nonzero only inside the single-particle excitation region. Thus only bare LO-phonons of large wave-vectors can be emitted. At finite temperatures, in principle, all values of q should contribute to the power loss in Eq.(5). At low temperatures, however, the main contribution is still expected to come from values inside the zero-temperature single-particle excitation region.

The dielectric constant $\epsilon(q, \omega)$ that screens the polarizability can be considered in two different extremes. The unscreened case [$\epsilon(q, \omega) = 1$] is expected to be valid at low electron densities, where screening does not play an important role. On the other extreme the static-screening approximation [$\epsilon = \epsilon(q, 0)$] should be adequate to describe high electron densities, because then the LO-phonon energy $\hbar\omega_{LO}$ is small compared to the typical energy scales associated with the electrons, namely the plasma energy $\hbar\omega_p$. A more realistic approximation would be to consider the full dynamic dielectric function, that is, to calculate $\epsilon(q, \omega = \omega_{LO})$. This should better represent the intermediate density region. Our numerical calculations explicitly test the quantitative validity of these approximations by using the full frequency dependent dielectric function in the theory.

III. Hot phonon effect

The actual situation for energy relaxation is somewhat more complex than is shown in Eq.(5), even for a

single electron, because the emission of an LO-phonon does not take energy out of the combined electron plus lattice system. The emitted LO-phonon must decay into acoustic phonon (via the anharmonic phonon-phonon interaction term), which then thermalizes with the surrounding heat bath fairly quickly. The decay of LO-phonons into acoustic phonons involves a finite LO-phonon lifetime, τ_{ph} . The significance of the hot phonon effect depends on the relative magnitudes of τ_{ph} , and the electronic relaxation time τ , becoming very important for $\tau < \tau_{ph}$.

This effect has been studied in great detail for bare LO-phonons^[17] and can be included, quite accurately, via a kinetic approximation. We assume that the relaxation of the LO-phonon can be completely described by the phonon lifetime τ_{ph} . In this situation, the average LO-phonon occupation numbers are not given by a Bose factor at the lattice temperature, since the emitted LO-phonons are no longer at equilibrium with the lattice. The dissipated power can be written as

$$P = \frac{\hbar}{N} \omega_{LO} n_T(\omega_{LO}) \sum_q \frac{R_q}{1 + \tau_{ph} R_q} \quad (7)$$

which, of course, is identical to Eq.(5) when the phonon relaxation time is zero: i.e. when the emitted LO-phonons decay instantaneously. When τ_{ph} is large, there could be a substantial hot (i.e. nonequilibrium) phonon bottleneck effect, causing a strong reduction in the cooling rate.

IV. Phonon models

We have studied several different models of the electron-phonon interaction. The finite cross section of the QWW acts to reduce the Coulomb interaction, and may also modify the LO-phonon spectrum through phonon confinement effects, consequently affecting the electron-phonon interaction.

The simplest approximation, which is widely used^[14,19], consists of considering bulk 3D-phonons, that is, to assume that the LO-phonons of the microstructure are the bulk ones, therefore ignoring any modification of the phonon spectrum introduced by the

finite width of the QWW. We shall refer to this model as the bulk model. A more realistic approach is to take into account the effects of the confining geometry on the LO-phonon spectrum. This can be done using two different macroscopic approaches to phonon confinement, the electrostatic or slab model and the mechanical or guided model, which differ essentially in the way the macroscopic boundary conditions are applied. In the electrostatic or slab model^[10,19] one applies boundary conditions on the electrostatic potential. Then for the LO-phonons, we have traveling waves in the direction of the wire (x), and standing waves in the transverse directions (y, z). This approximation is valid when the component of the polarization along the x -axis is much larger than its components in the confined directions [$k_x \gg \pi/L_y, \pi/L_z$]. In the mechanical or guided model^[11,20] the boundary conditions are applied to the atomic displacements at the interfaces. Then, the phonon wavevector directed along the quantum-wire axis is small relative to the sum of the two quantized phonon wavevectors in the other two directions [$(k_x)^2 \gg (\pi/L_y)^2 + (\pi/L_z)^2$].

For all these one-dimensional models, as we discussed before, the electron-phonon matrix element is given by Eq. (4) and contains the quantum form factor corresponding to the system considered.

IV.1. Bulk model

In the bulk model the electrons are confined in the quantum wire and the phonons are three-dimensional bulk phonons. The form factor for this system, for electrons in the lowest subband and assuming an infinite well potential can be written as^[21]

$$F_{1111}(q, L_y, L_z) = \int d\eta |G(\eta L_y/2)|^2 H(q, \eta, L_z) (\eta^2 + q^2)^{-1/2} \quad (8)$$

with

$$G(\xi) = \xi^{-1} \sin(\xi) [1 - (\xi/\pi)^2]^{-1} \quad (9)$$

and, using $\zeta \equiv L_z(\eta^2 + q^2)^{1/2}$

$$H(q, \eta, L_z) = \frac{2}{\zeta} + \frac{\zeta}{\zeta^2 + 4\pi^2} - \frac{32\pi^4(1 - e^{-\zeta})}{\zeta^2(\zeta^2 + 4\pi^2)^2} \quad (10)$$

IV.2. Confined models

The symmetry or the parity of the wave functions of the slab and mechanical models has to be opposite since in the slab model the electric potential has nodes at the interfaces, whereas in the mechanically confined model it is the electric field which is made to vanish at the interfaces. Then, mathematically, the difference between these two sets of modes is represented only by the interchange of the sine and cosine functions in the vibrational amplitudes of the modes^[20,22].

For the confined modes labeled by m and n , in both models, the form factor $F_{mn}(q)$ can be written as^[4,5]

$$F_{mn}(q) = \frac{32\pi}{L_y L_z} P_{mn}^2 \left[q^2 + \left(\frac{m\pi}{L_y} \right)^2 + \left(\frac{n\pi}{L_z} \right)^2 \right]^{-1/2} \quad (11)$$

where P_{mn} are the overlap integrals between the electronic ground state wave function and the confined modes, given by

$$P_{mn} = \int_{-1}^1 dy \int_{-1}^1 dz \cos^2\left(\frac{\pi}{2}y\right) \cos^2\left(\frac{\pi}{2}z\right) \phi_m(y)\phi_n(z) \quad (12)$$

with the functions $\phi_n(t)$ defined as $\phi_n(t) = \sin[(nt + \delta_n)\pi/2]$, for the slab modes, and $\cos[(nt + \delta_n)\pi/2]$ for the guided modes.

Since the only non-vanishing integrals of the type of Eq. (12) are those involving exclusively products of cosines, P_{mn} can be expressed as

$$P_{mn} = \frac{m\pi n\pi (4 - m^2)(4 - n^2)}{(8\pi)^2} \sin\left(\frac{m\pi}{2}\right) \sin\left(\frac{n\pi}{2}\right) \quad (13)$$

In order for P_{mn} to be nonzero for the slab modes, we must have both m and n odd integers, due to the functional dependence of the phonon wave function. The total matrix element is obtained performing the sum over these odd labels. The lowest order is $P_{11} = (8/3\pi)^2$. Since it can be shown that $|P_{13}| = 0.2 \times P_{11}$ and $|P_{ij}| < 0.04 \times P_{11}$ for $i, j > 1$, the dominant contribution to this sum is made by the mode with $m = n = 1$. Thus, we can to a good approximation consider only the lowest order overlap integral P_{mn} for the slab models. On the other hand, for the guided modes m and n must have even values and the

only non-vanishing term is $P_{mn} = 0.25$. Thus, in each case, we can consider only one value for P_{mn} , which corresponds to the lowest possible m and n for the model.

V. Results

In the rest of the paper, we present our numerical results for the intrasubband energy loss rates in GaAs QWW. We have used the following parameters: $m = 0.067 m_e$, $\alpha = 0.07$, $\hbar\omega_{LO} = 36.8 \text{ meV}$. We consider wires with lateral dimensions between 20 to 1000 Å, electronic densities of $10^3 - 10^7 \text{ cm}^{-3}$ and electron temperatures between 50 and 300K ($T_L = 0$ throughout). We have considered both classical and quantum cases for the three phonon confinement models described before. In the quantum systems, several different approaches to electronic screening were used: no screening [$\epsilon(q, \omega) = 1$], static screening [$\epsilon(q, \omega = 0)$] and full dynamic screening, with $\epsilon(q, \omega = \omega_{LO})$. In the dynamically screened case we have also considered the hot phonon effect, with values for τ_{ph} from 0 to 100 ps. Note that in the classical, unscreened and static screened cases we have not considered the hot phonon effect. The single subband approximation, used throughout this paper, is valid for the electron densities and the wire cross-sections chosen in our calculations.

In Fig. 1 we compare the results for all three models, for a given density, wire dimension, and dynamic screening ($\tau_{ph} = 0$ and 7 ps). Although, the experimental value for the hot phonon life-time in GaAs quantum wires is not yet known, 7 ps is the experimental 3D bulk value^[9]. In the scale of this figure, for each model, it is not possible to distinguish between the curves for the classical result, the unscreened or the dynamically screened system without hot phonon effect. For the smaller wire sizes and lower densities, all the results for the different approximations coincide with the corresponding classical results. The effects of the density and of the inclusion of the hot phonons are more pronounced for the slab modes and the values for the mechanically guided modes are much smaller. The results corresponding to the bulk model lie in between the two

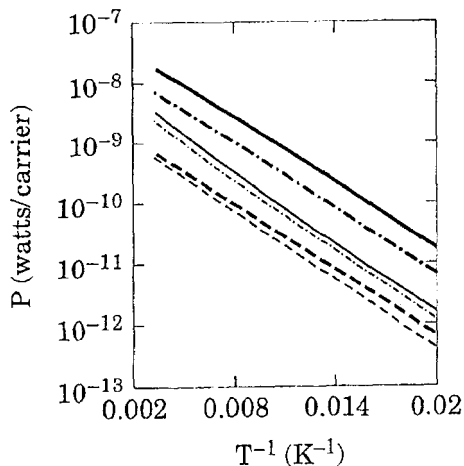


Figure 1: Power loss per carrier as a function of inverse electron temperature, for a quantum wire of lateral dimension $L_y = L_z = 100 \text{ \AA}$ and $N = 10^5 \text{ cm}^{-3}$. We have represented the dynamically screened results for the bulk phonons (dash-dotted curves), slab modes (solid curves) and guided modes (broken curves). In all the three models, the thick curves correspond to the case without hot phonons ($\tau_{ph} = 0$) and the thin curves to $\tau_{ph} = 7 \text{ ps}$.

confined models, but the behavior is qualitatively similar to that of the slab model.

For all the models, with or without phonon confinement, quantum statistics lowers the energy loss, even without the inclusion of screening^[4,5]. This is more noticeable for high densities and/or smaller wire cross section due to restrictions in the phase space for the electron scattering. As expected, screening usually further lowers the energy loss rate. For the dynamically screened systems and low densities, the results are slightly higher than those for the unscreened case (the so-called anti-screening effect). However, for high densities, dynamically screened results are almost the same as the statically screened case. The inclusion of phonon confinement does not change the overall behavior of the power loss curves, but only produces a rigid downward shift reducing the cooling rate. When we consider slab phonons, the loss is enhanced, while in the case of guided phonons, it is diminished. For all the studied cases, the energy loss is larger for smaller systems, although the activation energy for the curves is approximately the same. The results for $\log P$ vs $1/T$ are all approximately linear and parallel to each other, as can be seen in Fig. 1. This arises from the

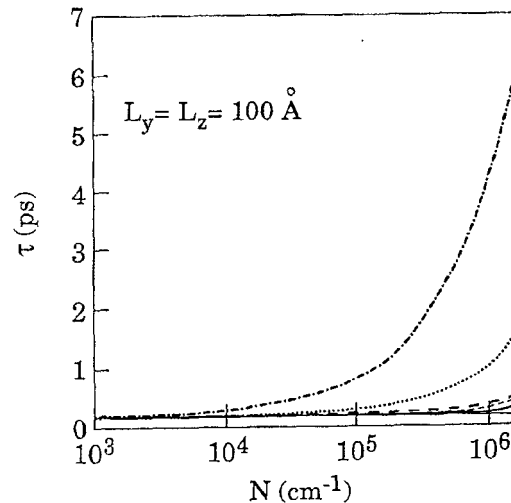


Figure 2: Electron relaxation time τ as a function of the electron density for $L_y = L_z = 100 \text{ \AA}$, as obtained from the power loss for the bulk model. Each curve corresponds to a different approximation, as described in the text: classical without screening (thin solid curve), quantum without any screening (thick solid curve), with static screening (thick dashed curve), with dynamic screening and no hot phonons (thin dashed curve), and including hot phonons, $\tau_{ph} = 1 \text{ ps}$ (dotted curve) and $\tau_{ph} = 7 \text{ ps}$ (dash-dotted curve).

fact that the Bose factor represents the dominant temperature dependence in Eq.(7). Then, we can write $P \approx (\hbar\omega_{LO}/\tau) \exp(-\hbar\omega_{LO}/k_B T)$, what allows us to define the electronic relaxation time τ .

The results for the electronic relaxation times τ can be calculated from the low temperature region. Fig. 2 represents τ vs density, for bulk phonons interacting with confined electrons and the different approximations considered, and $L_y = L_z = 100 \text{ \AA}$. For all approximations, when no hot phonons are considered, the unscreened case constitutes a good approximation for densities up to $4 \times 10^5 \text{ cm}^{-3}$. However, for larger densities, the static screening is a better approximation than the unscreened case. The effect of the inclusion of hot phonons is very strong even for small densities and wide quantum wires. Fig. 3a shows the dependence of the electronic relaxation time on the lateral wire dimension, for the bulk phonon model and a density of 10^5 cm^{-3} . For the larger wires the screening effects on the electronic relaxation time become more noticeable. Also, the "hot phonon" effect depends strongly on the electronic density, even for lower densities. This fact be-

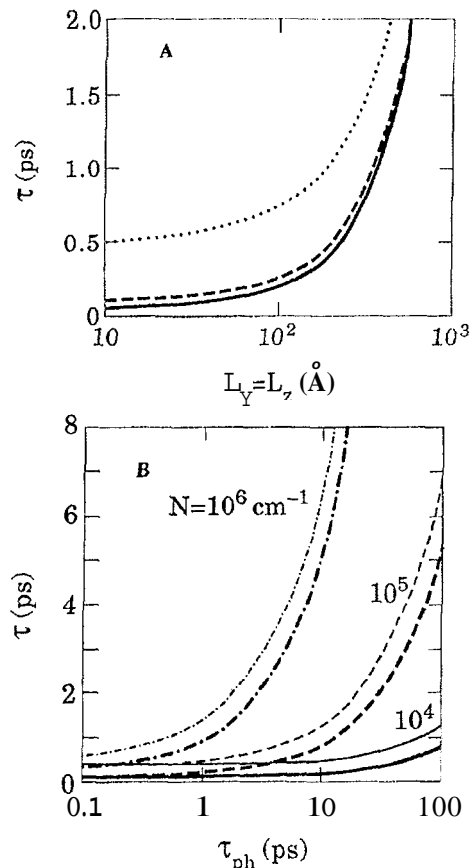


Figure 3: (a) Electron relaxation time τ for the bulk model, as a function of the lateral dimension of the wire $L_y = L_z$, for different densities, $N = 10^4$ and 10^5 cm^{-1} . In the scale of the figure, the results without considering hot phonons cannot be distinguished, for these densities (solid curve). The values for the dynamically screened results ($\tau_{ph} = 7 \text{ ps}$) are shown in the dotted curve ($N = 10^5 \text{ cm}^{-1}$) and the dashed one (10^4 cm^{-1}). (b) τ as a function of the phonon lifetime τ_{ph} , for different densities and lateral dimensions: $L_y = L_z = 50 \text{ \AA}$ (thick curves) and 200 \AA (thin curves).

comes more evident in Fig. 3b, where we show the correlation between the "hot phonons" in the bulk model and the dimensions of the wire for a number of different densities.

Qualitatively similar results^[5] are obtained for the electron relaxation times in the two models that include phonon confinement effects. Fig. 4a shows, for the three models, the calculated τ vs electron density, for $\tau_{ph} = 0$ and 7 ps and $L_y = L_z = 100 \text{ \AA}$. The slab and the guided model results were shifted so that all three models coincide in the low density region. The actual results for the two confined modes are shown in Fig. 4b. The values for the guided modes are more than

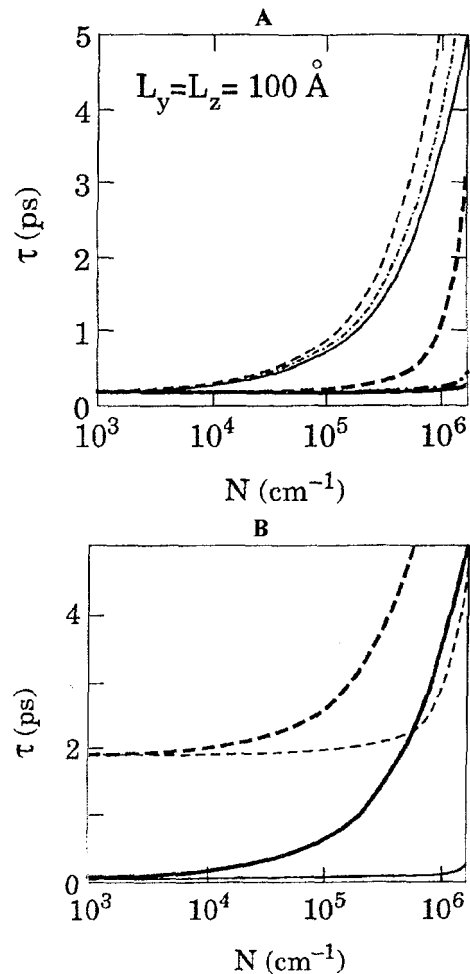


Figure 4: (a) Electron relaxation time τ as a function of the electron density for $L_y = L_z = 100 \text{ \AA}$, and the three phonon approximations: bulk phonons (dash-dotted curves), slab modes (solid), and guided modes (dashed). The thick (lower) curves correspond to ($\tau_{ph} = 0$) and the thin ones to $\tau_{ph} = 7 \text{ ps}$. The curves for the two confined models were made to coincide with the bulk results, for the low densities. The actual values of the two confined modes are shown in (b), where the upper curves correspond to the guided modes and the lower ones to the slab modes.

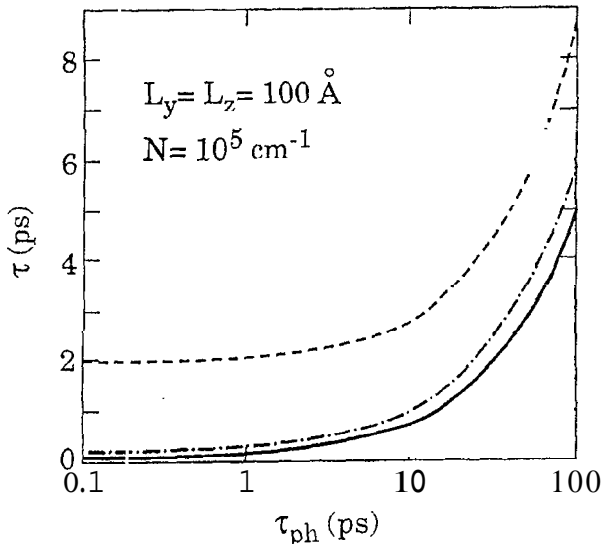


Figure 5: Electron relaxation time τ as a function of the phonon lifetime τ_{ph} for wire width $L_y = L_z = 100 \text{ \AA}$ and $N = 10^5 \text{ cm}^{-1}$, for the guided modes (broken curve), the slab modes (solid curve) and the bulk phonons (dot-dashed curve).

an order of magnitude larger than the slab or the bulk results, indicating a much slower relaxation.

In Fig. 5 we show the actual results for τ_{ph} , for the three models, for a density of 10^5 cm^{-1} and $L_y = L_z = 100 \text{ \AA}$. The overall dependence on τ_{ph} for the three cases is the same, although the guided mode results are slower, especially for low values of τ_{ph} .

VI. Conclusion

In summary, we have calculated the hot electron energy relaxation rate in GaAs quantum wires for intrasubband relaxation via bulk and confined LO-phonon mode emission in the electric quantum limit. Our calculation includes electron and phonon confinement effects, quantum degeneracy, dynamic screening and hot phonon bottleneck effect. We compare the results for bulk phonons interacting with confined electrons with the two standard phonon confinement models, namely the slab and the guided mode models, and find, consistent with the quantum well situation, that the guided (mechanical) modes produce more than an order of magnitude slower energy relaxation than the slab (electrostatic) modes for intrasubband relaxation processes. The results for the slab modes are close to our calcu-

lated bulk results. Hot phonon bottleneck is found to be the single most important physical mechanism in our calculations provided $\tau_{ph} > 1 \text{ ps}$. Our calculated relaxation rates are comparable to those found in quantum wells.

For all the one-dimensional systems considered, when the dimensions are small ($50 \text{ \AA}/50 \text{ \AA}$), it constitutes a good approximation to neglect screening for electron densities below 10^5 cm^{-1} . For higher densities, screening effects are important with static screening becoming a good approximation at very high densities. For larger systems ($1000 \text{ \AA}/1000 \text{ \AA}$), the screening effects cannot be distinguished except in the case where hot phonon effects are included. Another important result is that the hot phonon effect depends on the electronic density. For $\tau_{ph} = 0$, the low density electron system can be regarded as unscreened and non-degenerate, which makes the power loss per carrier practically independent of density. With the inclusion of the hot phonon effect ($\tau_{ph} = 7 \text{ ps}$), when the density varies from 10^3 to 10^4 cm^{-1} , the value of τ increases by a factor of two.

At the present time, there is no available experimental information on hot electron energy relaxation in semiconductor quantum wires. Our hope is that our extensive numerical investigation of the cooling rate will stimulate experimental activity in the subject.

Acknowledgments

This work is supported in part by FAPESP (Fundação de Amparo à Pesquisa do Estado de São Paulo, Brasil), CNPq (Conselho Nacional de Desenvolvimento Científico e Tecnológico, Brasil), US-ARO and US-ONR.

References

1. See for example, *Hot Carriers in Semiconductor Nanostructures: Physics and Applications*, edited by J. Shah (Academic Press, Boston, 1992) and the Proceedings of the International Conference on Hot Carrier in Semiconductors, published in

- Semicond. Sci. Technol. 7 (1992) and Solid State Electronics 32 (1989) and 31 (1988).
2. S. Das Sarma, in *Hot Carriers in Semiconductor Nanostructures: Physics and Applications*, edited by J. Shah (Academic Press, Boston, 1992) p. 53, and references therein.
 3. S. Das Sarma., V. B. Campos, M. A. Stroschio and K. W. Kim, Semicond. Sci. Technol. 7, 860 (1992).
 4. V. B. Campos and S. Das Sarma, Phys. Rev. B 15, 3898 (1992).
 5. V. B. Campos, S. Das Sarma and M. Stroschio, Phys. Rev. B 46, 3849 (1992).
 6. V. B. Campos, S. Das Sarma and M. Stroschio, Phys. Rev. B, (1994) in press.
 7. S. Das Sarma and V. B. Campos, Phys. Rev. B 47, 3728 (1993).
 8. A. R. Goni et al., Phys. Rev. Lett. 67, 3298 (1991).
 9. J. A. Kash, J. C. Tsang and J. M. Hvam, Phys. Rev. Lett. 54, 2151 (1985); J. A. Kash, S. S. Jha and J. C. Tsang, *ibid.* 58, 1869 (1987).
 10. J. K. Jain and S. Das Sarma, Phys. Rev. Lett. 62, 2305 (1989); K. Mori and T. Ando, Phys. Rev. B 40, 6175 (1989); S. Rudin and T. L. Reinecke, Phys. Rev. B 41, 7713 (1990); L. Wendler and R. Pechsted, Phys. Stat. Solidi (b) 141, 129 (1987).
 11. B. K. Ridley, Phys. Rev. B 39, 5282 (1989); M. Babiker, J. Phys. C 16, 683 (1986); B. K. Ridley and M. Babiker, Phys. Rev. B 43, 9096 (1991).
 12. S. M. Kogan, Fiz. Tverd. Tela 4, 2474 (1963) [Sov. Phys.-Solid State 4, 1813 (1963)].
 13. S. Das Sarma, J. K. Jain and R. Jalabert, Phys. Rev. B 41, 3561 (1990) and references therein.
 14. S. Das Sarma and B. A. Mason, Ann. Phys. (NY) 163, 78 (1985).
 15. P. F. Maldague, Surf. Sci. 73 296 (1978); S. Das Sarma., Phys. Rev. B 33, 5401 (1986).
 16. V. B. Campos, O. Hipólito and R. Lobo, Phys. Rev. B 15, 4234 (1977); P. F. Williams, A. N. Bloch, *ibid.* B 10, 1097 (1974).
 17. P. J. Price, Physica B&C 134b, 155 (1985); P. Kocivar, *ibid.* 134b, 164 (1985).
 18. P. J. Price, Ann. Phys. 133, 217 (1987); Surf. Sci. 113, 199 (1982).
 19. M. A. Stroschio, Phys. Rev. B 40, 6428 (1989).
 20. M. A. Stroschio et al. Superlatt. and Microstruct. 10, 55 (1991).
 21. M. H. Degani and O. Hipólito, Phys. Rev. B 35, 9345 (1987); V. B. Campos, M. H. Degani and O. Hipólito, Solid State Comm. 79, 473 (1991).
 22. S. Rudin and T. L. Reinecke, Phys. Rev. B 41, 7713 (1990).